ZH-154
AUGUST 1961

CONTRACT NOw60-0494-d

NOX

CONVAIR-SAN DIEGO CONVAIR DIVISION GENERAL DYNAMICS CORPORATION

STUDY OF HIGH SPEED PROJECTILE IMPACTS, LOADS, AND MOTIONS AT WATER ENTRY

GENERAL DYNAMICS | CONVAIR

TABLE OF CONTENTS

LIST OF FIGURES

LIST OF TABLES

FOREWORD

This report presents results from an experimental investigation of high-speed (to supersonic air velocities) water entry impacts of conical-nosed missile-type projectiles. Axial impact acceleration measurements have been obtained by employment of specially-developed, self-contained FM telemetering instrumentation, and the experimental data have been compared with theory. The report is submitted to the Bureau of Naval Weapons in fulfillment of Contract NO 60-0494-d with General Dynamics/Convair.

SUMMARY

This report presents results from an experimental investigation of high-velocity water entry impacts of 60-degree total apex angle conical-nosed projectiles. Salient results from the program are summarized as follows:

1. Projectiles with 1-inch and 2-inch diameter bodies have been fired vertically into water at air Mach numbers ranging from 0.4 to 1.0 (vertical velocities from 395 to 1120 fps).

2. Specially-developed accelerometer and sub-miniature epoxy-potted FM telemetering instrumentation were employed within the projectile body for the measurement of axial accelerations during water impact.

3. Water impact acceleration-time histories were recorded successfully during five tests with velocities ranging from 396 to 838 fps and with the maximum axial accelerations varying from 1530 to 6000 g's. It has been shown that the impact acceleration measurements are in good approximate agreement with the Pierson immersing-wedge theory, but that the experimental measurements fall considerably lower than the Shiffman-Spencer theory.

4. Water impact pressure measurements were obtained in the far field (1.2 feet from the point of impact) which, together with theory, permit extrapolation of the experimental data to higher velocities.

It is believed that significant advancements have been made with modest funding in the development of the self-contained FM telemetering instrumentation and in the employment of this instrumentation to measure impact accelerations at entry velocities as large as 838 fps. Previous acceleration measurements from known model tests were made at entry velocities less than 200 fps. Recommendations are made for follow-on work to improve the design and reliability of the self-contained instrumentation and to extend the experiments to both higher velocities and to other nose configurations.

RECOMMENDATIONS FOR CONTINUED WORK

As a result of the findings of this experimental investigation the following recommendations are made for continued work:

1. That further development of the self-contained subminiature FM transmitter be undertaken with emphasis on the improvement of signal strength, durability and the reduction of microphonic resonances. It is proposed that four advanced transmitters be constructed and calibrated thoroughly.

2. That the experimental measurement of axial accelerations during vertical water entry with the 60-degree conical-nosed projectile be extended from a velocity of 838 fps attained in the present experiments to supersonic water entry air velocities ranging between 1200 and 2000 fps. It is proposed that a correlation of these data be made with theory.

3. That experimental investigations be made of scale-effects on water entry accelerations by testing three different sizes of projectiles and further that the effects of oblique water entry angles on the accelerations be investigated.

4. That water entry impact acceleration measurements be made for other nose shapes including contemporary nose forms, and special forms to give alleviations of the impact accelerations, and that theory be extended or formulated to apply for these configurations.

INTRODUCTION

The development of high performance air-to-underwater missiles which are capable of entering the sea intact, at supersonic air Mach numbers (velocities of 1200 to 2000 feet per second, for example), and of subsequently completing prescribed missions underwater has been hampered severely by the lack of experimental water impact acceleration data at high water entry velocities. A missile that is underdesigned structurally could be debilitated or demolished beyond practical use during the violent water impact at high velocities. A structurally overdesigned missile would have its performance penalized directly due to any amount of excessive weight.

As of the time of writing of this report, no known previous water impact acceleration time-history measurements have been obtained at velocities exceeding a few hundred feet per second using essentially a rigid body projectile. A limited number of tests have been made at high entry speeds using full scale prototype missiles, but large structural deflections and structural resonances of the fabricated bodies have largely obscured physical interpretation of the data, and have prevented application of the results to the design of other missiles having different body forms and structural configurations.

The present experimental investigation was undertaken with the quite worthy objective of making a major advancement in the technology - obtaining essentially rigid body water impact acceleration measurements at speeds up to those exceeding sonic velocity. This advancement had become feasible from a technical point of view largely because of recent important developments in the subminiaturization of electronic components. This would now permit the construction of a special small-size FM telemetering oscillator that could be contained within a small, rigid body, hydrodynamic model. The program should be regarded as an exploratory endeavor, on a limited budget, to fulfill the above objective. We regret to report that the single transmitter which was developed did fail, short of the objective. However, we are pleased to report that water impact acceleration data were measured successfully at velocities up to air Mach number 0.75.

DISCUSSION

A. Test Equipment

The experimental investigation described in this report consisted basically of firing two projectiles of different sizes vertically into the water. The purposes of the investigation were to measure the water entry impact accelerations and to observe the pitching motions of the projectile at high velocities (260 fps to 1120 fps).

A sizeable portion of the program was spent developing new and modifying existing equipment including the projectiles, compressed gas gun, water tank, instrumentation, etc. These components are discussed in detail in the following paragraphs.

(1) Projectiles

Two projectiles of different sizes were used, having nominally 1-inch and 2-inch diameters (Figure 1). Both projectiles incorporated the same nose configuration, (i.e., a conical nose with a 60-degree total included angle). As may be noted in Figure 1, the nose cone of each model was constructed of solid aluminum in order to minimize structural deformations that would influence the accuracy of the transducer. Note, also, that none of the projectiles have incorporated stabilizing appendages.

The main body of the projectile was constructed of fiberglass. The purpose of this non-metallic material was to permit the transmission of the radio signal from the sub-miniature transmitter encased within.

The rear of the projectile incorporated a steel stud which served the dual purpose of preventing the instrumentation from shifting and holding the plastic diaphragm in place during firing.

The smaller projectile was completely filled with instrumentation, and, as a result, its center of gravity (percentage of length aft of nose apex) was taken as

a standard for all projectiles. The c.g. for the large projectiles was adjusted to this standard with lead ballast. The projectile parameters are tabulated in Table I.

TABLE I

PROJECTILE PARAMETERS

Projectile	Diameter (inches)	Gross Wt. (lbs)	Location of c.g. Aft of Nose Apex (inches)
1	0.92	0.34	3.4
2	1.88	2.72	6.8
3	1.88	1.77	6.8

(2) Gun

A pneumatic gun was used to accelerate the projectile to the high velocities for water impact (Figure 2). A single gas chamber was used with interchangeable barrels in order to accommodate the different projectile sizes (Figure 3). The gas chamber was sealed from the barrel by a diaphragm attached to the rear face of the projectile. When the chamber pressure was sufficient to burst the diaphragm, the projectile was fired. During these tests, a combination of 1, 2, 3 and 5 thousandths of an inch thick Mylar plastic diaphragms were used. The gun was designed for a working pressure of 6000 psi; however, the present tests required maximum pressures of only 2000 psi. Dry nitrogen was used as a driving gas in the cylindrical shaped chamber (approximately 3 feet long, 6 inches I.D.). The barrels were smooth bore with a length of 10 feet.

(3) Tank

Because higher test velocities and larger projectiles were utilized during this program, it was necessary to obtain a larger tank than had been previously used. A 20 foot length of 2 feet diameter pipe was secured for this purpose. This tank was erected in a vertical position directly below the gun (Figure 4).

Originally three 6 inch by 5 feet windows of Gaphite were installed at the upper end of the tank. Later the window size was reduced. Plexiglas was installed in place of Gaphite and a "shock mounting" type of installation was used. A length of 6 inch diameter hose was hung co-axially within the tank below the test section. This was done as a deceleration aid and to contain the unstable projectile until it came to rest at the bottom of the tank. Water in the tank was filtered and maintained at a constant level.

(4) Instrumentation

(a) Photography

High speed photographs were taken through the center window of the tank (Figure 5). High intensity flood lights were installed at the windows on each side of the camera as well as at the top of the tank. The light output of these units was increased by stepping up the voltage to the bulbs.

The camera used was a Photo-sonics 4B (35 mm movie) (Figure 6). Initially the camera was operated at the rate of 2000 pictures per second. At the higher test velocities the camera was operated at 2500 pictures per second. A 9° shutter and Eastman Tri X film were used. At 2500 frames per second, the exposure time was 0.01 milliseconds.

(b) Velocity

The projectile velocity was measured with the aid of two photo-electric cells spaced 3 feet apart along the flight path. The time required for the projectile to travel this distance was recorded by an electronic counter, and the velocity was computed. The output signal from both photo-electric cells was also recorded on tape along with the other data. The upper interrupter was also used to trigger the oscilloscope during the recording of data.

(c) Pressure Transducer

An Atlantic Research LD 80 hydrophone was placed in the tank to sense the peak pressure transmitted to the water by the projectile at entry impact. In an effort to isolate the transducer from vibrations of the tank and other interferences, it was imbedded in a five pound block of lead. This in turn was suspended from the tank wall in such a manner as to be facing the center of the tank, 10 inches below the water surface and 10 inches radially from the point of impact.

The output of the transducer was coupled to an amplifier through a cathode follower matching circuit and then recorded on tape.

(d) Accelerometer and Transmitter

An Endvco Model 2225 accelerometer was bolted securely to the back side of the nose cone in order to enable it to sense the impact deceleration with minimum structural response. The output of this unit is approximately flat (10%) from 5 cps to 15 kc with its first resonance frequency at 80 kc. The unit is capable of recording up to 20,000 g's (shock) with an amplitude linearity of 1%. The output itself is nominally 6 peak millivolts per peak g.

The accelerometer, used to translate the physical shock forces into proportional electrical signals, is basically a charge generator. Such a device has no significant power output and so must be followed by an impedance changing circuit (Figure 7).

A two transistor, Darlington emitter follower, combined with bootstrapping feedback is used to accomplish the high input impedance and long time constant required by the transducer. The output of the impedance changer modulates an RF oscillator.

The transistor, RF oscillator, was designed in grounded base configuration for maximum center frequency stability. By applying the modulation signal so that the voltage across the base-collector diode changes, the capacitance across the diode junction follows proportionally. Inasmuch as this capacitance appears

across the oscillator tank circuitry the frequency of oscillation is FM'd at a rate determined by the signal from the transducer. An FM, RF signal is generated directly from the circuitry into space. Only a small portion of the RF energy is released from the oscillator coil as it is in toroid form for microphonic stability of the tank.

At the incept of oscillator design, the 2N384 transistor was the most acceptable state-of-the-art item for both oscillator and impedance changer, due to its frequency characteristics. The internal construction of this transistor, however, has undesirable capacity changes, upon shock-impact. The micro and pico transistors which are solid packaged and now off-the-shelf available, have good physical stability as well as acceptable pulse and frequency characteristics.

Off the shelf, encapsulated, R.F., micro-toroids combined with micro or pico transistors would reduce physical capacitance changes within the oscillator circuitry and provide more accurate shock-impact data.

By combining certain portions of the impedance changer and oscillator circuits, three parts may be eliminated. This combining action would also allow more efficient use of the power drain, which would raise the power output and result in a more desirable signal to noise ratio at the receiver. In future work, therefore, the means for significant transmitter improvements will be available.

Sub-Miniature Transmitter

(e) Receiver and Tape Recorder

A standard telemetering receiver (Nems Clark) was used to receive and demodulate the signal from the projectile. This signal was then recorded on an Ampex 814 tape recorder which had a frequency response to 0 to 70 kc at ± 1 db. All data was put on tape because of the greater reliability and versatility.

(f) Oscilloscope

The data recorded on the magnetic tapes were played back to a Model 545A Tektronic oscilloscope fitted with a polaroid camera. The data, therefore, was ultimately recorded by photographic techniques.

B. Testing Procedure

The testing procedure utilized during this program involved the following specific steps:

1. The FM telemetering transmitter and power supply were installed in the projectile and connected to the accelerometer.

2. Milar plastic diaphragms of predetermined thickness (depending upon the test velocity desired) were attached to the rear face of the test model.

3. The FM receiver was tuned to the center frequency of the transmitter. The photo-electric cells were energized and the electronic counter placed on stand-by.

4. The model was placed in the barrel of the gun and the barrel attached to the chamber.

5. Dry nitrogen was introduced into the chamber of the gun. As the chamber pressure approached the desired value, the tape recorder, photographic lights, and the high speed camera were started.

6. At the predetermined chamber pressure the plastic diaphragms failed and the projectile was accelerated down the barrel.

7. As the model left the gun barrel, it de-energized the first photo-electric cell thereby starting the electronic counter.

8. Before impacting the water, the model de-energized the second photo-electric cell and thereby turned off the electric counter.

9. At the instant of water contact, the impact acceleration was transmitted to a receiving antenna adjacent to the path of the model. Also the impact pressure imparted to the water was measured by the pressure transducer. The signals from the two photo-electric cells, the accelerometer, and the pressure transducer were recorded as time histories on magnetic tape.

10. The projectile, after passing through approximately 12 inches of water, entered a 6 inch diameter hose which served to guide it into the retrieving container at the bottom of the tank.

11. The projectile was retrieved from the container and the test procedure repeated.

C. <u>Problem Areas</u>

(1) A weak area was created at the top of the entry tank due to the three large window cut-outs. Upon water impact, this area of the tank expanded slightly causing the windows to shatter. The windows consisted of transparent plastic (Gaphite) attached directly to the tank. Gaphite was initially chosen as the window material because of its excellent high temperature properties. These properties were desirable because of the heat produced by the photographic lamps. Gaphite, however, is a rather brittle material and could not tolerate the stresses resulting from the flexure of the tank.

The problem was solved by replacing the Gaphite glazing with plexiglas, reducing the over-all dimensions of the window openings, and adopting a more resiliant type of mounting.

(2) The test projectiles were unstable because stabilizing appendages were not incorporated. The instability was not apparent during the short flight in air, but was significant in water. During preliminary runs with a dummy model the missile trajectory was diverted to the extent that the missile contacted the side of the tank at high velocity. Damage to both the model and the tank was sustained.

In an effort to contain the projectile during deceleration, a six inch diameter rubber hose was suspended in the center of the tank and below the test area. The model was contained within the hose and arrested at the bottom of the tank. No further problems due to instability were encountered.

(3) The FM transmitter was the one component of instrumentation requiring development. Due to the pioneering aspects and the stringent physical requirements placed upon this component, its development was quite involved. The most severe problem was procurement of suitable electronic components. It was necessary that these components exhibit proper electronic properties and physical size as well as the structural integrity to withstand the applied loads without damage or variation in electrical values.

The transmitter circuitry was designed to utilize the latest sub-miniature components that were commercially available. (Improved components were under development but were commercially unavailable at the time.) The resulting transmitter met the response characteristic requirements, but produced a somewhat marginal signal to noise ratio. The internal structural integrity of certain components presented reliability problems and ultimately resulted in failure of the transmitter.

(4) A minor problem with the operation of the receiver was encountered. The receiver required a finite period of time to stabilize electrically upon receiving a radio signal. This period of time was longer than that required for the projectile to travel from the gun barrel to the surface of the water. (The gun barrel was constructed of steel and therefore was opaque to the radio signal.) The impact acceleration data are therefore superimposed upon the low frequency oscillation

of the receiver output voltage. This problem was not too serious because the receiver oscillation frequency was considerably below that of the data and was easily recognized.

D. Experimental Data and Methods of Analysis

(1) Impact Accelerations

Testing was initiated with the 1 inch projectile. Impact accelerations were measured during eight firings. On preparation for the ninth shot the transmitter was found to be totally inoperative. Subsequent analysis of the data records indicated a progressive failure of the transmitter over several previous runs. The net result was that usable data was obtained on five of the eight runs. All eight of these original records are presented in Figure 9 (a). These records show the entire signal output from the time the transmitter left the muzzle until it was drowned out in the water.

Since the projectile velocity was known after each run, time from muzzle to water contact could be calculated. A portion of the trace on each side of the water contact point was expanded with respect to time and is shown in Figure 9 (b). Figure 9 (c) and (d) are further time expansions of (b).

From the expanded traces (i.e., Figure 9 (b), (c) and (d)) the impact is more apparent. These traces were read measuring the downward excursion from the mean trace level. The slope of the mean trace level is due to the low frequency oscillations of the receiver. These measurements are recorded in Table II. The calibrations below the photos in Figure 9 suggest a linear output from the data system. This is true for all components except the transmitter. It is shown in the transmitter calibration curve (Figure 10) that the output is very close to linear except at the higher "g" levels. It was found convenient to use the linear calibration and then enter the curve in Figure 10 for the corrected value.

The data tabulated in Table II is plotted in Figure 11. Along with these data are plotted the experimental points by Mosteller (Ref. 1) and the two theoretical

curves. These are represented by the equations

$$\eta = 7.61 \times 10^{-3} \dot{y}_o^2$$

(Pierson, Ref. 2)

and

$$\eta = 15.4 \times 10^{-3} U_o^2$$

(Schiffman & Spencer, Ref. 3) .

This will be discussed more completely in a later section.

TABLE II

TABULATION OF IMPACT DATA*

Test No.	Trace Deflection Centimeters	Impact g's	Impact g's (corrected)	Impact Velocity Feet/Second
1	0.8	2450	2600	496
2	0.6	1840	1880	655
3	1.6	4900	6000	838
4	0.9	1380	1380	396
5	1.0	1532	1532	424
6				461
7				454
8				623

* Other tests were made after failure of the transmitter in which an impact velocity of 1120 fps was attained.

** Taken from Figure 10.

(2) Water Pressure

During all runs the pressures imparted to the water by the projectile at impact were measured and recorded. The amplitudes of these pressures were obtained by measuring from the oscilloscope photos the displacement of the trace from the zero point. These amplitudes are shown in Figures 12 and 13. Through these data have been plotted the curves represented by the generalized equation

$$p = KV^2$$

where K has been computed from the empirical values of pressure and velocity. It is felt that the absolute values of these pressures are not valid. However, no attempt has been made to correlate these pressures with theory due to the large effect the air blast from the gun might have as well as the structural effect of the tank. It is believed that in the case of the one inch projectile a correlation can be made with the accelerations measured concurrently with these pressures. This can be seen in Figure 14.

(3) Impact Velocity

The method used to measure projectile velocity resulted in an average velocity over the three foot travel. Thus the velocities computed are not impact velocities but rather the velocity at a point 3-1/2 feet above the water surface. It is felt, however, that this discrepancy is negligible.

(4) Missile Motions

Projectile instability was not apparent in the high speed photos taken during testing (Figure 8). These photos covered an area about 2 inches above the water surface and about 10 inches below. It was apparent, however, that the projectile was unstable. In approximately five feet of travel in the water it diverged one foot from centerline, at which time it contacted the tank wall.

(5) Correlation of Experimental Data with Theory

It was desired to determine the degree to which theory would substantiate the data obtained in the water impact experiments. In view of the contractor's experience in use of the Pierson immersing wedge theory of Reference 2 for computing the impact loads of seaplanes, a similar approach was formulated here.

The Pierson theory gives

$$\eta = \frac{\ddot{y}}{g} = \frac{\Sigma F_y}{W} = \frac{C_L S \frac{1}{2} \rho \dot{y}^2}{W}$$

The buoyancy force and projectile weight were assumed to be negligible in comparison to the very large hydrodynamic force and were omitted from the above equation. It was also assumed that $\dot{y}$ is constant and equal to $\dot{y}_o$ during the time period until the shoulder of the cone becomes wetted. The experimental data and analog computer solutions of the impact acceleration time histories verify that both of the above assumptions are quite reasonable and should not give significant error. Water added mass effects during the impact were neglected in the above equation and References 4 and 5 show that this omission is perfectly reasonable because of the insignificant magnitudes of the acceleration modulus. It was desired to solve for the maximum value of the water entry load factor and therefore the wetted area in the above equation was taken as the nose frontal area to the shoulder of the cone, S.

Values of C_L given by Pierson in Reference 2 were derived for essentially two-dimensional wedge shapes, and data given in Reference 6 which compare values of C_L for two-dimensional wedges and three-dimensional axially-symmetrical cones were employed to establish a correction factor K_1 for the basic Pierson equation. Although the data in Reference 6 are for 60-degree half apex

angle bodies, they were assumed to be applicable for the present 30-degree half-apex angle. Thus, by averaging the pressure distribution curves given on page 217 of Reference 6

$$K_1 = \frac{C_{L_{cone}}}{C_{L_{wedge}}} \cong \frac{3.0}{5.0} = 0.6$$

The Pierson theory for a wedge gives

$$C_{L_{wedge}} = 2.16\left(\frac{90}{\beta} - 1\right)^2 \tan\beta = 2.16\left(\frac{90}{60} - 1\right)^2 \tan 60° = 0.94$$

and then for the cone

$$C_{L_{cone}} = K_1\, C_{L_{wedge}} = 0.56$$

The frontal area of the cone is

$$S = \pi r^2 = \frac{\pi\,(0.460)^2}{144} = 4.62 \times 10^{-3}\ \text{ft}^2$$

also

$$\frac{1}{2}\rho \cong 1\ \text{slug/ft}^3 \text{ and } W = 0.340\ \text{lb.}$$

Finally, the Pierson theory with use of the above correction factor K_1 gives

$$\eta = \frac{C_{L_{cone}}\, S\, \frac{1}{2}\rho\, \dot{y}_o^2}{W} K_1 = \frac{0.56(4.62)(10^{-3})(1)\,\dot{y}_o^2}{0.340} = 7.61 \times 10^{-3}\, \dot{y}_o^2$$

The agreement of the experimental water impact measurements with the Pierson theory is shown in Figure 11.

The experimental data are also compared in Figure 11 with a second approximate theory by Shiffman and Spencer given on page 390 of Reference 3. It should be noted that Shiffman and Spencer do give an exact solution for the vertical water entry accelerations of a cone at constant velocity, but that the calculation would require employment of a digital computing machine and for this reason use of the exact equation was beyond the scope of the present project. The approximate Shiffman-Spencer equation is as follows:

$$\eta = \frac{1}{W}\left(3K\,\sigma \tan^3 \frac{\theta}{2} U_o^4\, t^2\right)$$

K was read from Graph 1, page 403 of Reference 3 to equal 1.06. t was assumed to equal the time elapse until the shoulder of the cone becomes wetted, or

$$t = \frac{\dfrac{r}{\tan \frac{\theta}{2}}}{U_o}$$

The substitution of this expression into the basic Shiffman-Spencer equation gives

$$\eta = \frac{1}{W}\left(3K\,\sigma \tan \frac{\theta}{2}\right)(U_o^2\, r^2) = \frac{1}{0.340}(3)(1.06)(1.94)(\tan 30°)\left(\frac{0.460}{12}\right)^2 U_o^2$$

$$= 15.4 \times 10^{-3}\, U_o^2$$

The Shiffman-Spencer equation gives values of η which are approximately twice as great as given by the Pierson theory. It should be noted that values of K given by Shiffman and Spencer for use with their approximate equation were derived from only four experimental data points measured at relatively low water impact velocities by Japanese investigator Watanabe in 1930.

SYMBOLS

β	Deadrise Angle from Horizontal
C_L	Lift Coefficient $= \dfrac{F_y}{1/2\, \rho\, \dot{y}^2\, S}$
F_y	Force in y Direction (vertical)
g	Acceleration of Gravity
K, K_1	Constants
η	Load Factor $\ddot{y}/g$
θ	Total Vertex Angle of Cone
p	Pressure
r	Radius of Wetted Portion of Cone
ρ, σ	Mass Density of Water
S	Frontal Wetted Area
t	$\dfrac{\dfrac{r}{\tan\frac{\theta}{2}}}{U_o}$
U_o	Velocity at Impact
V	Velocity
W	Weight
$\dot{y}_o$	Velocity at Impact
$\dot{y}$	Velocity
$\ddot{y}$	Acceleration

REFERENCES

1. Mosteller, G.G., "Axial Deceleration at Oblique Water Entry of 2-Inch Diameter Models with Hemisphere and Disk Cylinder Noses," NAVORD Report 5424, February 1957.

2. Pierson, John D., "The Penetration of a Fluid Surface by a Wedge," Stevens Institute of Technology, Experimental Towing Tank Report No. 381, July 1950 (Sherman M. Fairchild Publication Fund Paper No. FF-3, Institute of the Aeronautical Sciences).

3. Schiffman, Max & Spencer, D.C., "The Force of Impact on a Cone Striking a Water Surface (Vertical Entry)," Comm. Pure & Applied Math., Vol. IV, No. 4, November 1951.

4. Iversen, H.W. & Balent, R., "A Correlating Modulus for Fluid Resistance in Acceleration Motion," Journal of Applied Physics, Vol. 22, March 1951.

5. Oversmith, Robert H., "Cavitation of Axially Symmetrical Bodies in Accelerating Motion," Journal of Ship Research, Vol. 4, No. 3, December 1960.

6. Cox, R. N., & Maccoll, J. W., "Recent Contributions to Basic Hydroballistics," Symposium on Naval Hydrodynamics Nat. Academy of Sciences - NRC Publication 515, 1957.

ACKNOWLEDGEMENT

Acknowledgement is given to Mr. George Silberberg at NOTS China Lake and Mr. Darrell Lassiter of Photo-Sonics, Inc., for their technical assistance in the field of high speed photography.

FIGURE 1. DRAWINGS OF PROJECTILES

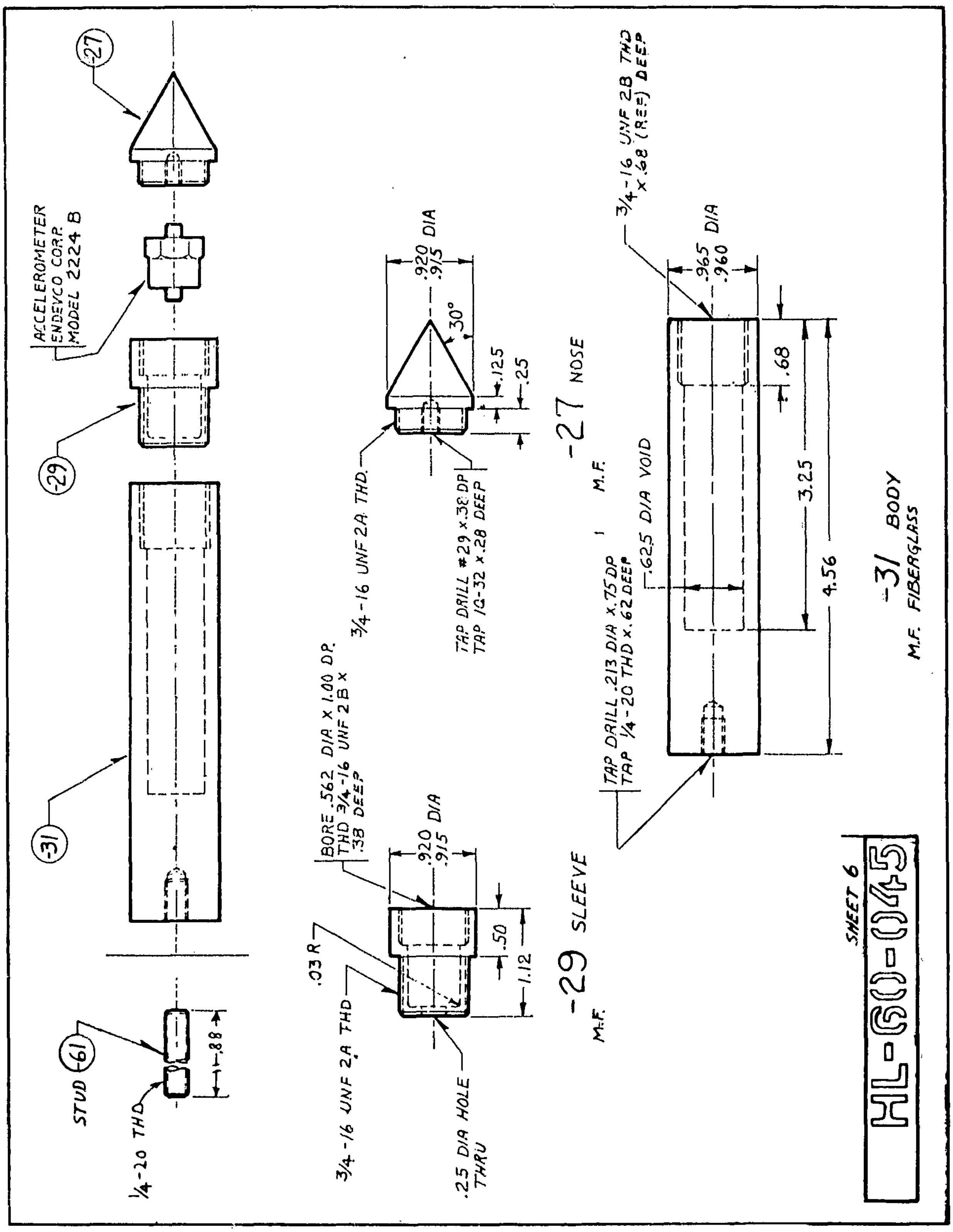

FIGURE 1. DRAWINGS OF PROJECTILES (Cont)

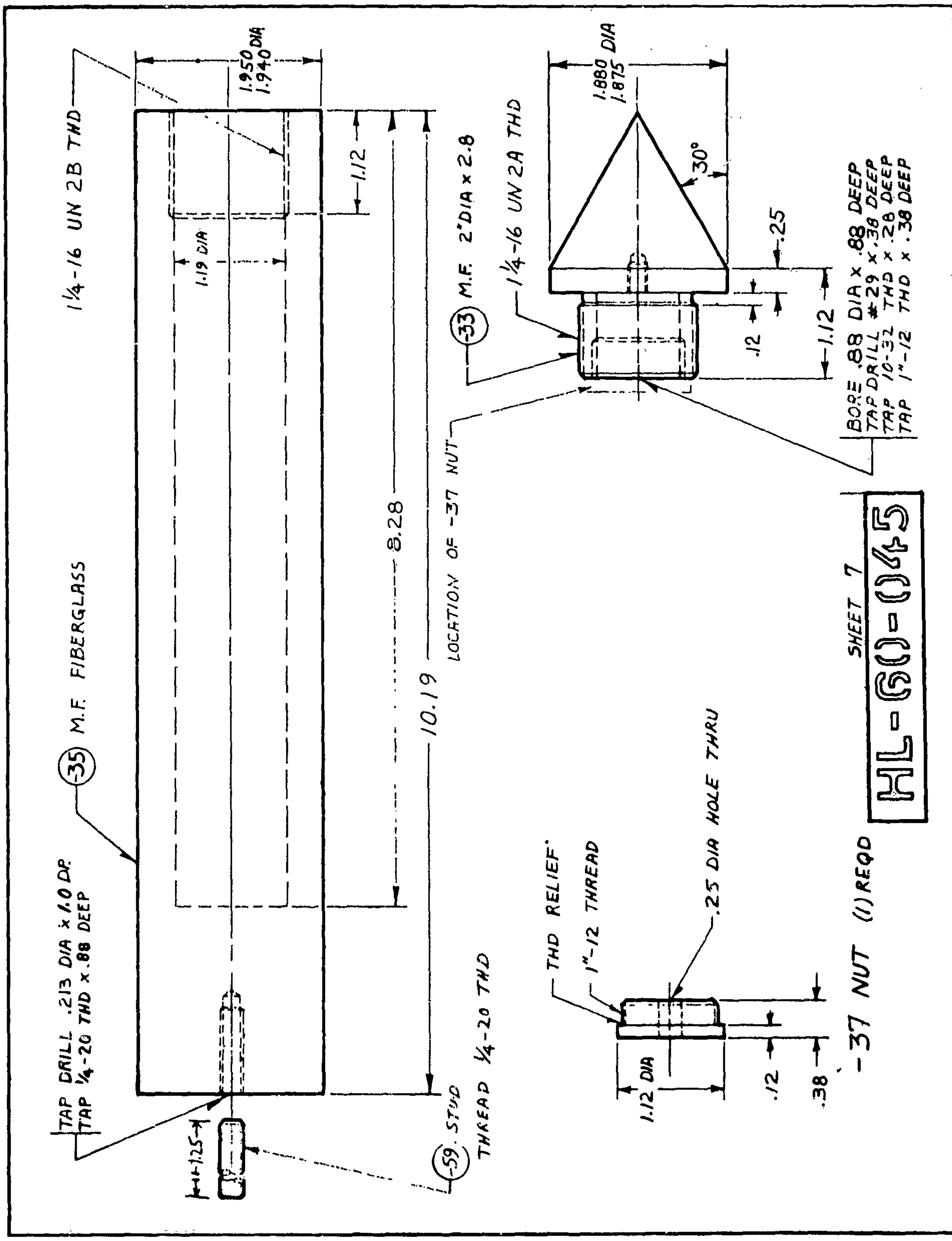

FIGURE 2. GUN AND TOWER

FIGURE 3. PROJECTILE IN GUN

FIGURE 4. TEST RIG

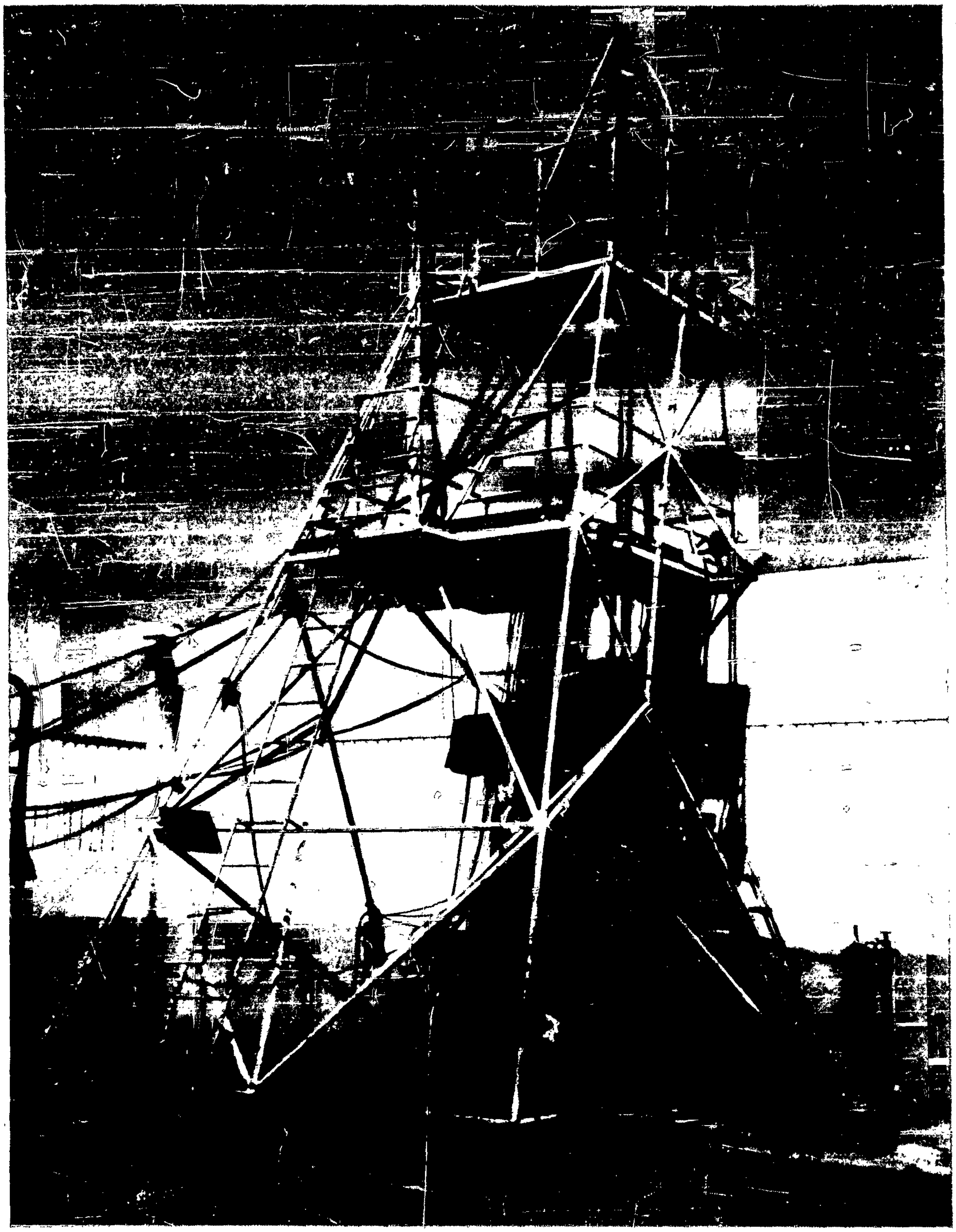

FIGURE 5. CAMERA AND TANK

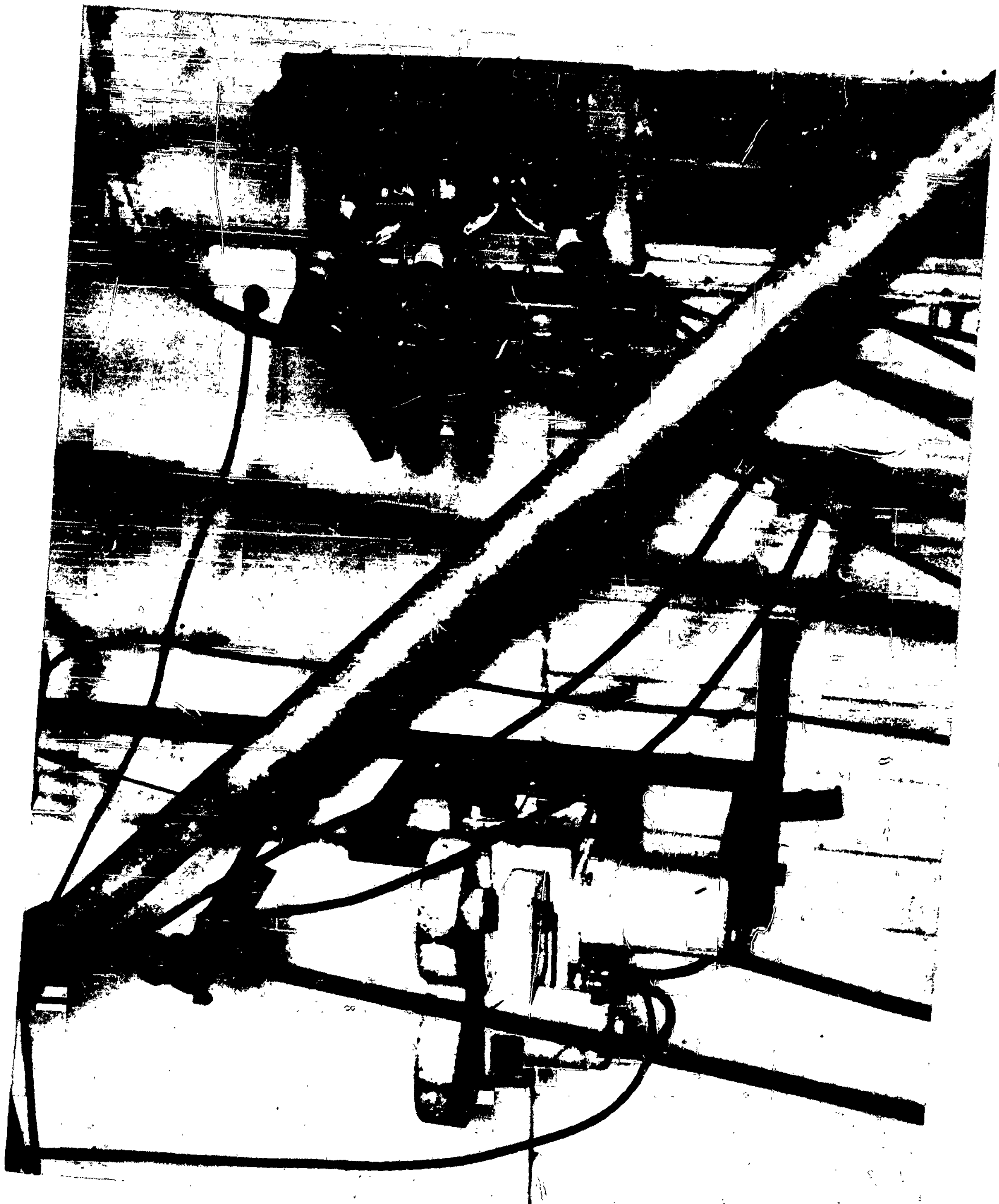

FIGURE 6. CAMERA

FIGURE 7. SCHEMATIC OF TELEMETERY TRANSMITTER

Signal Centered at 50-55 MC (≅)

Frequency Modulated

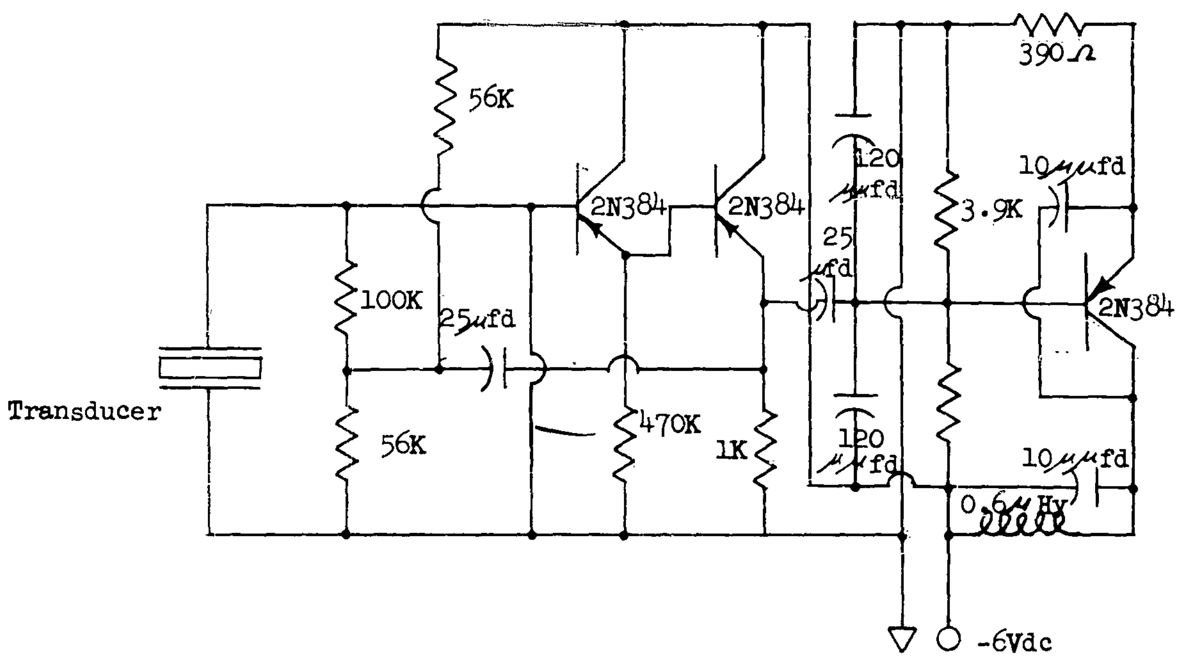

FIGURE 8. WATER ENTRY PHOTOGRAPHS

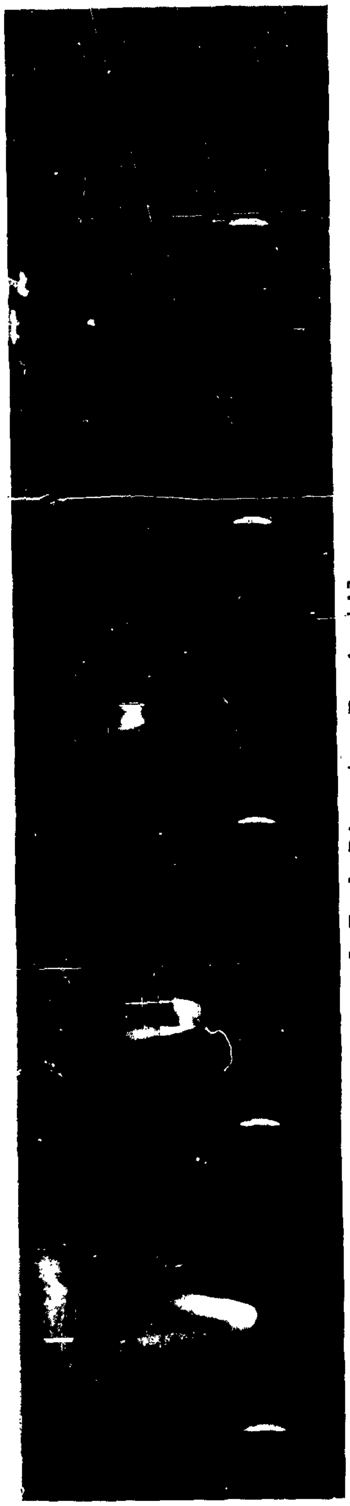

1-Inch Diameter Projectile
Weight = 0.34 lb. Velocity = 454 ft/sec

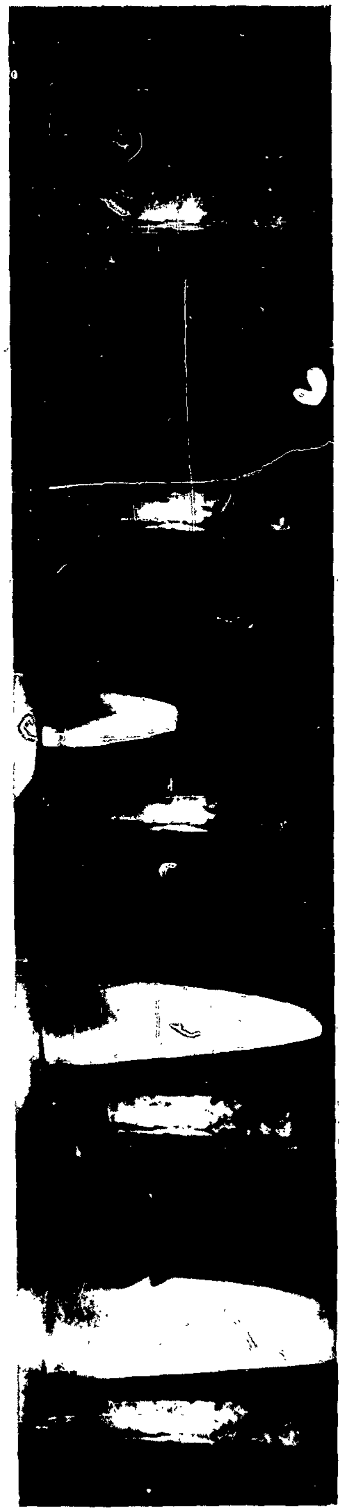

1-Inch Diameter Projectile
Weight = 0.34 lb. Velocity = 1080 ft/sec

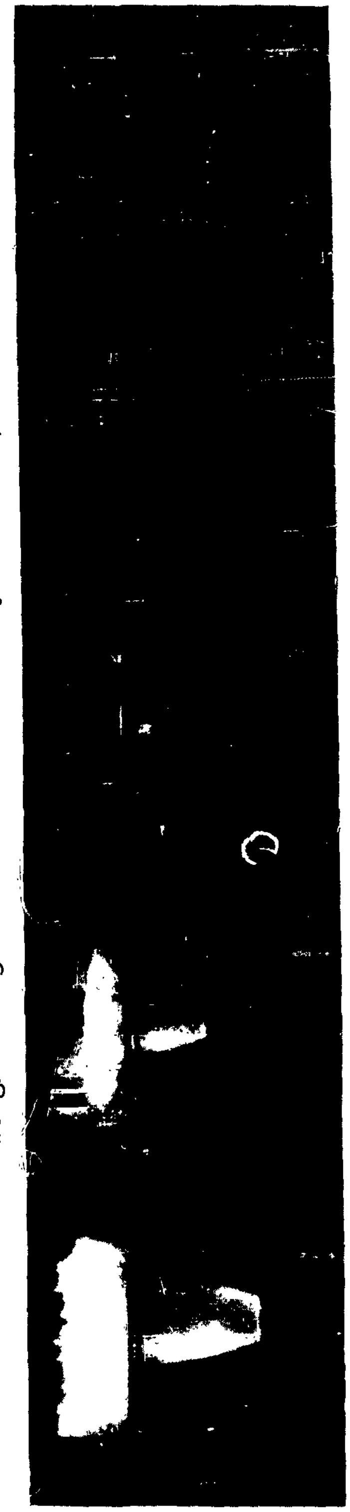

2-Inch Diameter Projectile
Weight = 2.72 lb. Velocity = 353 ft/sec

FIGURE 9. ORIGINAL ACCELEROMETER RECORDS

Explanatory Diagrams	Test No. 1 Velocity = 496 ft/sec	Test No. 2 Velocity = 655 ft/sec
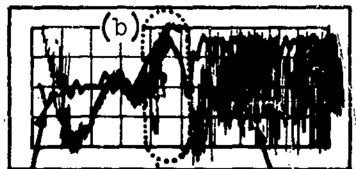 (b) receiver signal strength, data signal (a) expanded to + signal	 (a) 1532 g's/cm 0.0 ms delay, 2 ms/cm	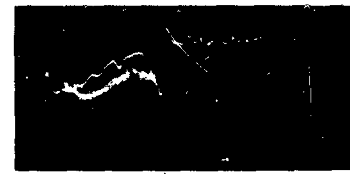 (a) 1532 g's/cm 0.0 ms delay, 2 ms/cm
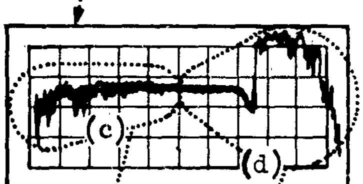 (c) (d) (b) expanded to	 (b) 3064 g's/cm 8.8 ms delay, 0.2 ms/cm	 (b) 3064 g's/cm 6.4 ms delay, 0.2 ms/cm
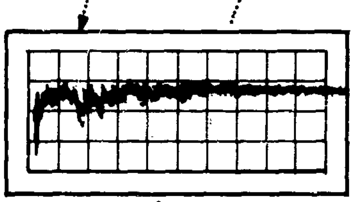 (c)	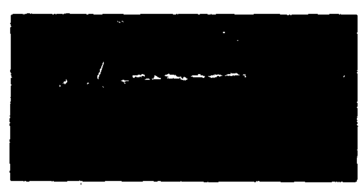 (c) 3064 g's/cm 8.8 ms delay, 0.1 ms/cm	 (c) 3064 g's/cm 6.4 ms delay, 0.1 ms/cm
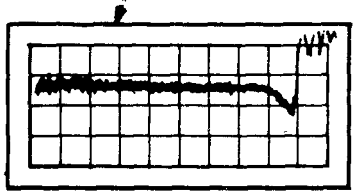 (d)	 (d) 3064 g's/cm 9.8 ms delay, 0.1 ms/cm	 (d) 3064 g's/cm 7.4 ms delay, 0.1 ms/cm

Note: Each grid square is one square centimeter.

FIGURE 9. ORIGINAL ACCELEROMETER RECORDS (Cont)

Test No. 3
Velocity = 838 ft/sec

(a) 1532 g's/cm
0.0 ms delay, 2 ms/cm

(b) 3064 g's/cm
4.8 ms delay, 0.2 ms/cm

(c) 3064 g's/cm
4.8 ms delay, 0.1 ms/cm

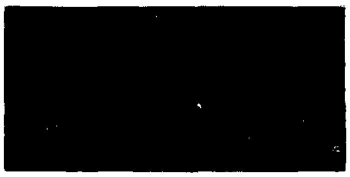

(d) 3064 g's/cm
5.8 ms delay, 0.1 ms/cm

Test No. 4
Velocity = 396 ft/sec

(a) 1532 g's/cm
0.0 ms delay, 2 ms/cm

(b) 1532 g's/cm
11.6 ms delay, 0.2 ms/cm

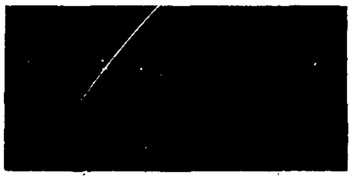

(c) 1532 g's/cm
11.6 ms delay, 0.1 ms/cm

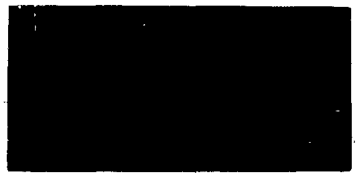

(d) 1532 g's/cm
12.6 ms delay, 0.1 ms/cm

Test No. 5
Velocity = 424 ft/sec

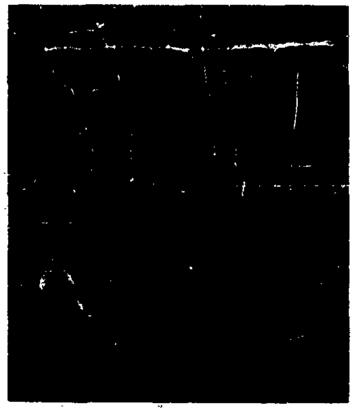

(a) 1532 g's/cm
0.0 ms delay, 1.0 ms/cm

(b) 1532 g's/cm
11.2 ms delay, 0.2 ms/cm

(c) 1532 g's/cm
11.2 ms delay, 0.1 ms/cm

(d) 1532 g's/cm
12 ms delay, 0.1 ms/cm

Note: Each grid square is one square centimeter.

FIGURE 9. ORIGINAL ACCELEROMETER RECORDS (Cont)

Test No. 6
Velocity = 461 ft/sec

1532 g's/cm
0.0 ms delay, 2.0 ms/cm

Test No. 7
Velocity = 454 ft/sec

1532 g's/cm
0.0 ms delay, 2.0 ms/cm

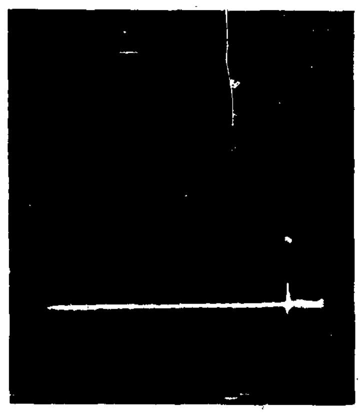

Projectile Ringing
Natural Frequency
1.0 ms/cm

Test No. 8
Velocity = 623 ft/sec

1532 g's/cm
0.0 ms delay, 2.0 ms/cm

Note: Each grid square is one square centimeter.

FIGURE 10. TRANSMITTER CALIBRATION CURVE

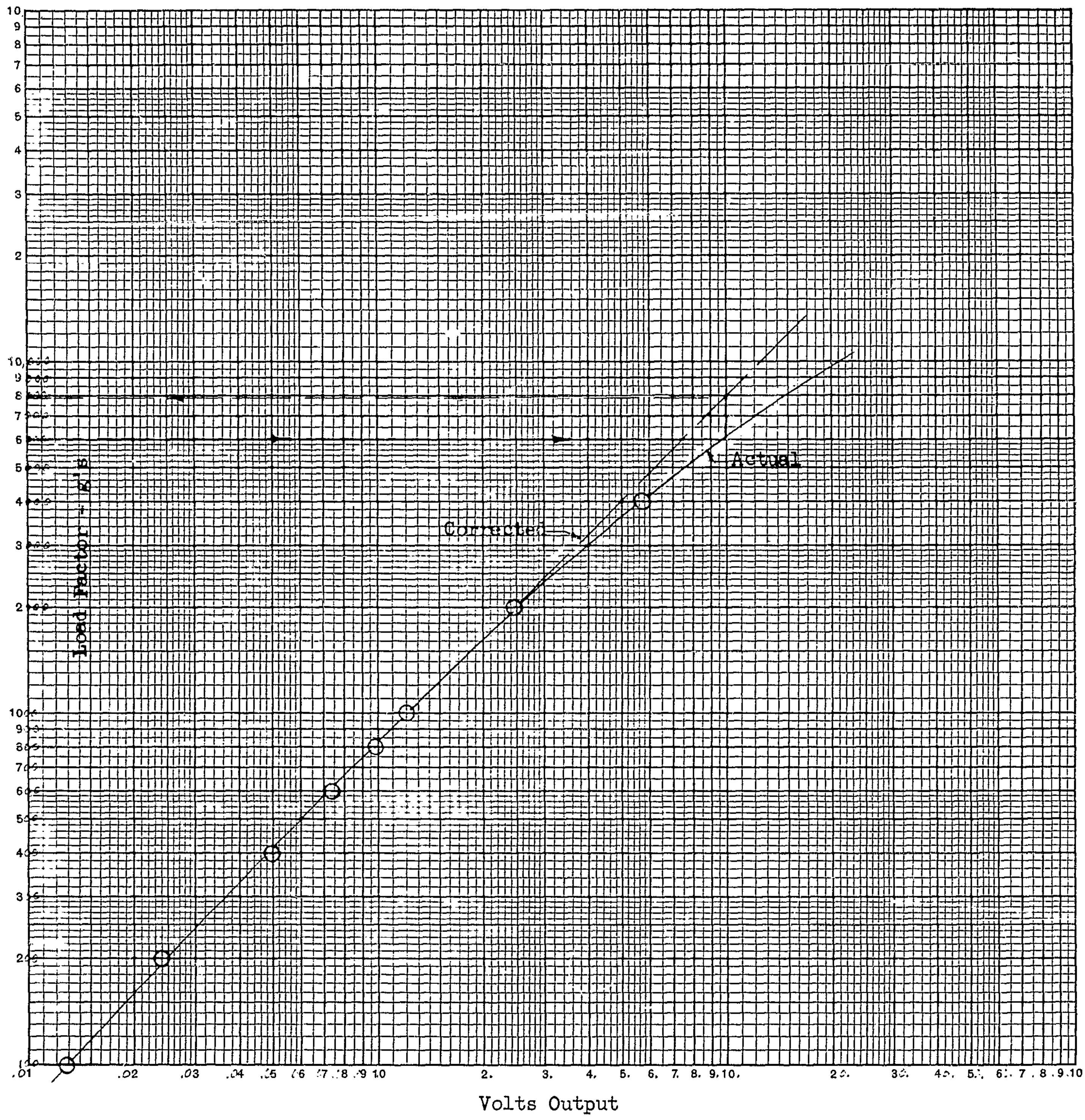

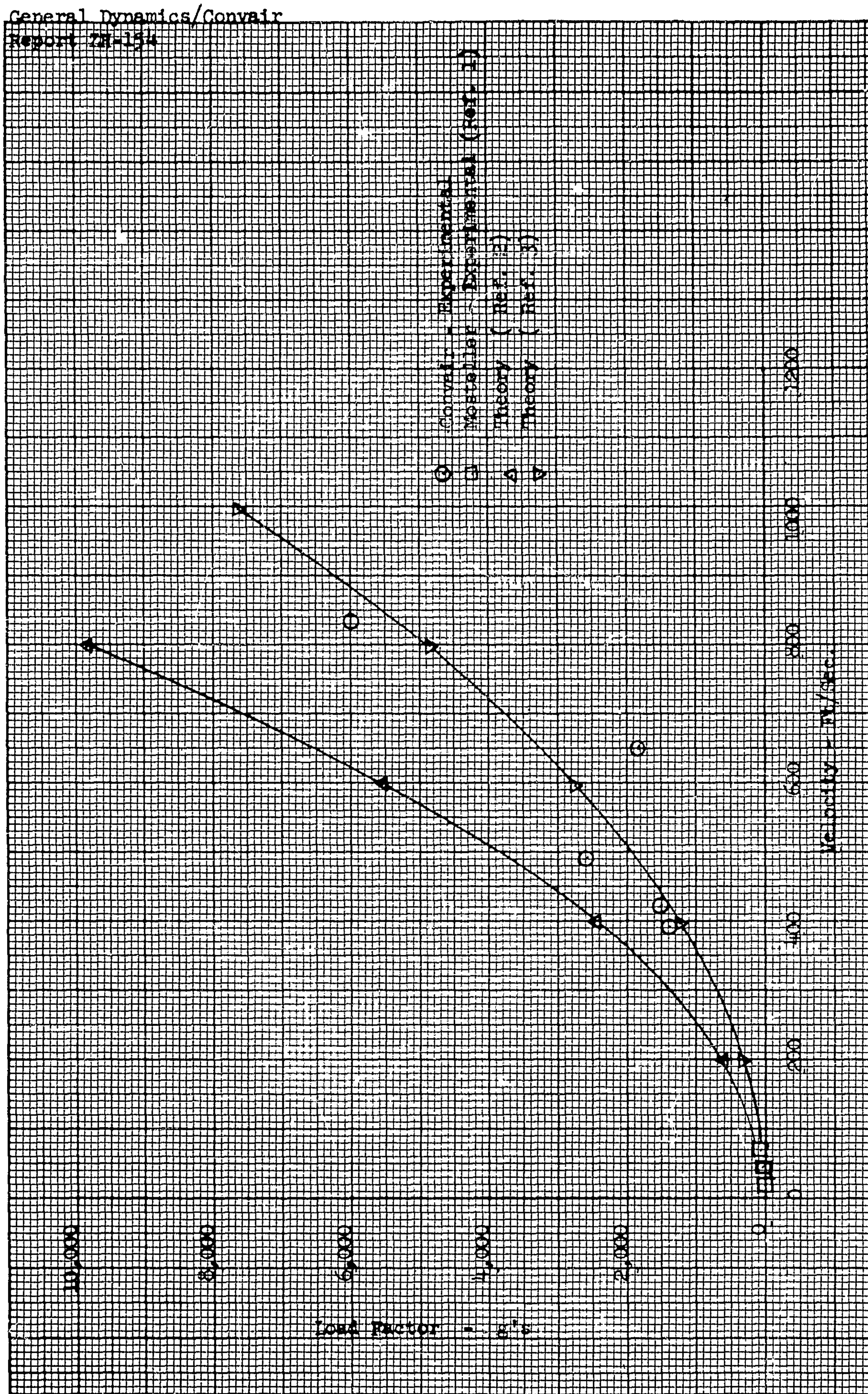

FIGURE 11. IMPACT ACCELERATIONS FOR 1-INCH PROJECTILE

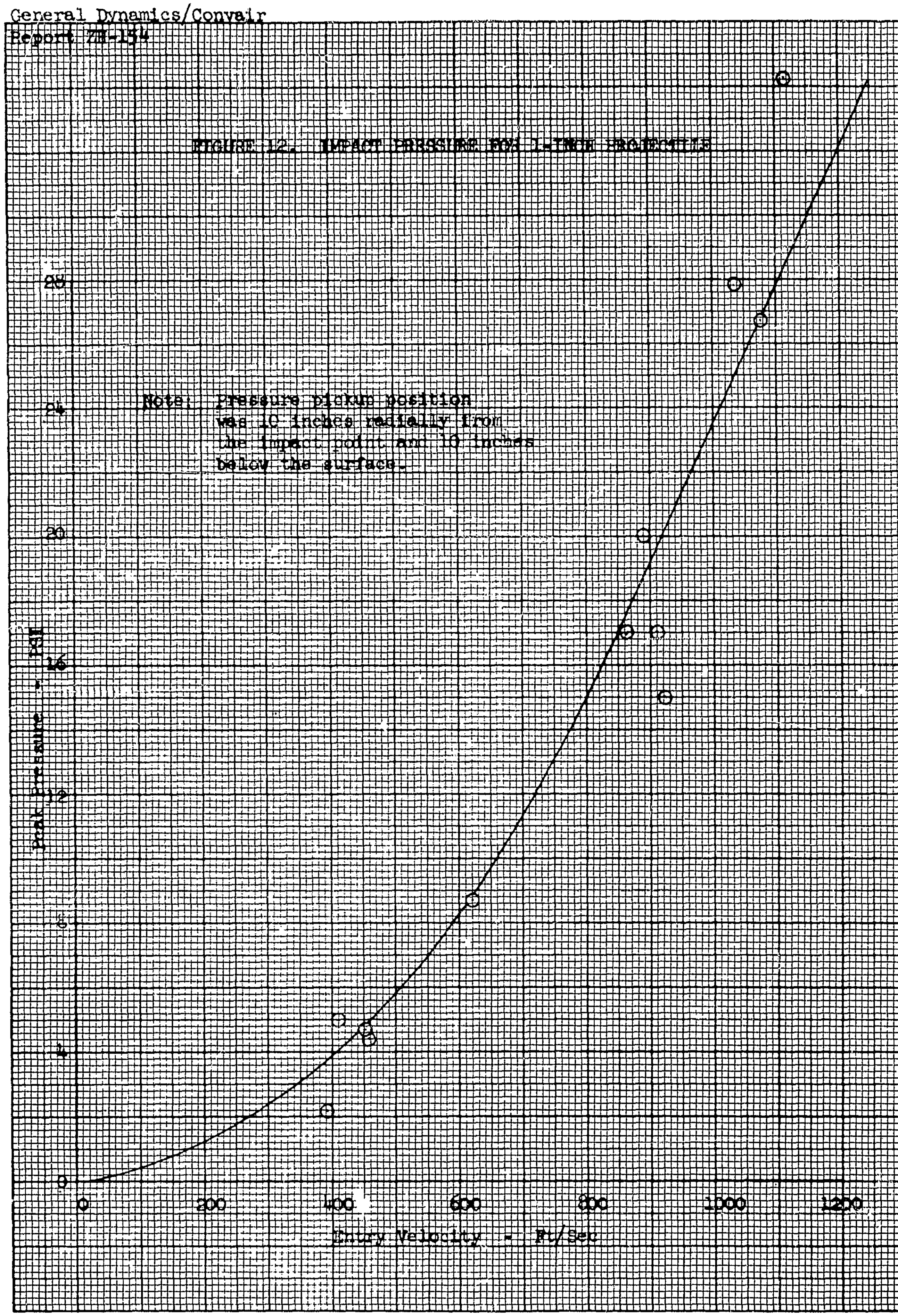
FIGURE 12. IMPACT PRESSURE FOR 1-INCH PROJECTILE
Note: Pressure pickup position was 10 inches radially from the impact point and 10 inches below the surface.
Peak Pressure - PSI
0
4
8
12
16
20
24
28
0
200
400
600
800
1000
1200
Entry Velocity - Ft/Sec

FIGURE 13. IMPACT PRESSURE FOR 2-INCH PROJECTILE

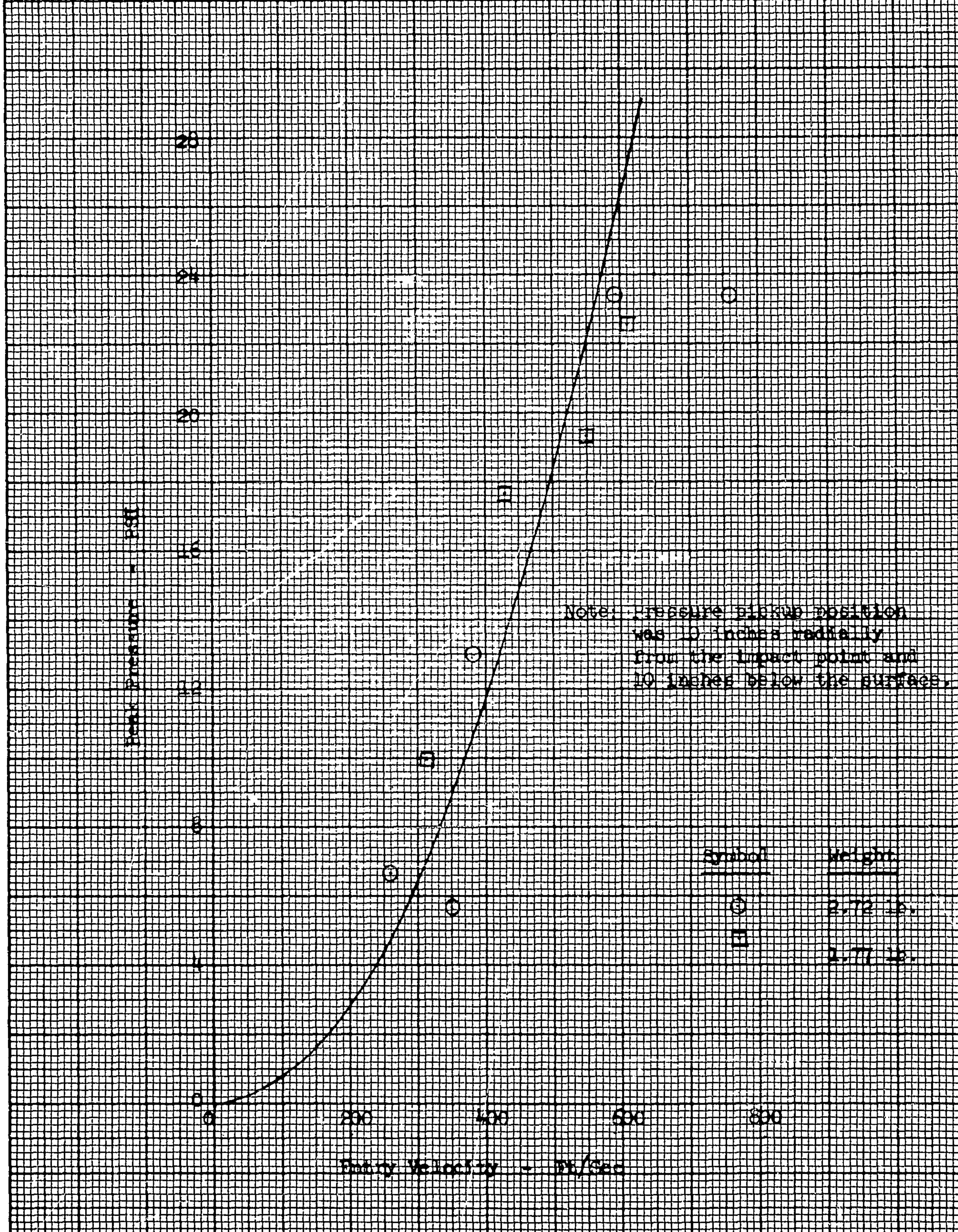

FIGURE 13. IMPACT PRESSURE FOR 2-INCH PROJECTILE

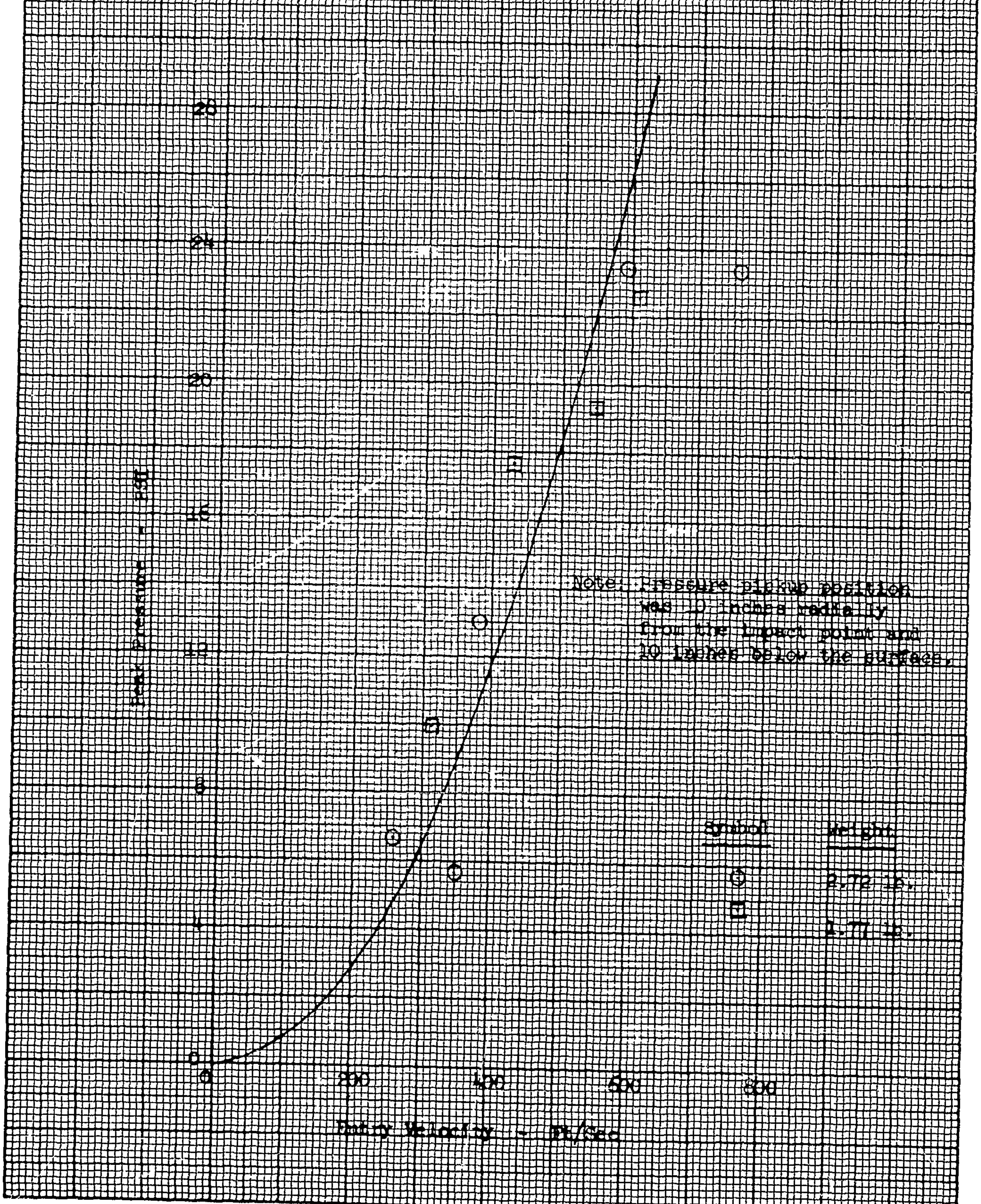

FIGURE 14. IMPACT PRESSURES VS ACCELERATIONS FOR 1-INCH PROJECTILE

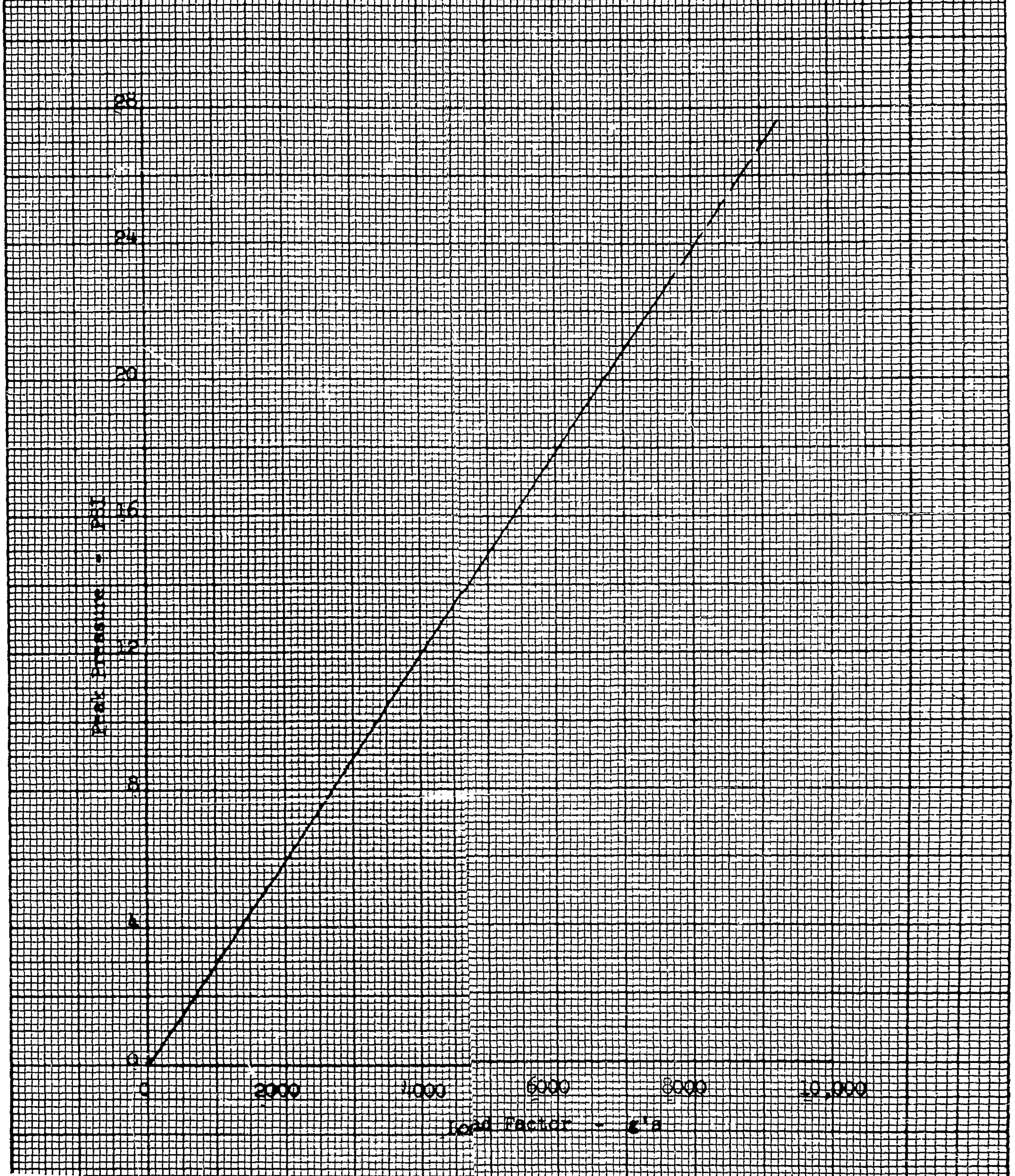

EP #558 (68)